Applied Catalysis B: Environmental 340 (2024) 123225

Contents lists available at ScienceDirect

Applied Catalysis B: Environmental

journal homepage: www.elsevier.com/locate/apcatb

Magnetic field facilitated electrocatalytic degradation of tetracycline in wastewater by magnetic porous carbonized phthalonitrile resin

Junling Zeng [a], Wenhao Xie [a], Ying Guo [b], Tong Zhao [b], Heng Zhou [b,*], Qiaoying Wang [c], Handong Li [d,e], Zhanhu Guo [d], Ben Bin Xu [d], Hongbo Gu [a,*]

[a] Shanghai Key Lab of Chemical Assessment and Sustainability, School of Chemical Science and Engineering, Tongji University, Shanghai 200092, PR China
[b] Institute of Chemistry, Chinese Academy of Sciences, Beijing 100190, PR China
[c] State Key Laboratory of Pollution Control and Resource Reuse, Shanghai Institute of Pollution Control and Ecological Security, College of Environmental Science and Engineering, Tongji University, Shanghai 200092, PR China
[d] Mechanical and Construction Engineering, Faculty of Engineering and Environment, Northumbria University, Newcastle Upon Tyne NE1 8ST, UK
[e] College of Materials Science and Engineering, Taiyuan University of Science and Technology, Taiyuan 030024, PR China

ARTICLE INFO

Keywords:
Tetracycline
Electrocatalytic degradation
Carbonized phthalonitrile resin
Magnetic field effect
Spin polarization

ABSTRACT

Herein, the magnetic field facilitated electrocatalytic degradation of tetracycline is reported for the first time. A magnetic porous carbonized phthalonitrile resin electrocatalyst has been prepared through directly annealing phthalonitrile monomer, polyaniline coated barium ferrite and potassium hydroxide. The tetracycline degradation percentage (DP%) by such electrocatalyst is significantly increased up to 37.42% under magnetic field with the optimal pH value of 5.0 and bias voltage of 1.0 V (*vs.* SCE). The mechanism of this phenomenon is explained by the spin-selective electron removal process in the reaction between metal-oxygen species and tetracycline on the electrocatalyst. The comparison of degradation pathways for tetracycline with and without magnetic field confirms the improvement of tetracycline DP%. This work opens a new direction for the application of an external magnetic field in the electrocatalytic degradation of antibiotics in wastewater.

1. Introduction

The annual usage of antibiotics is extremely large all over the world. However, a large amount of antibiotics cannot be absorbed by creatures and enters the environment, which causes undeniable threats to human life [1]. Tetracycline, as a type of antibiotics, can be utilized to treat microbial diseases (*e.g.*, cholera, malaria, acne, *etc*.) in humans and animals [2]. Unfortunately, with excellent solubility in water, tetracycline is hard to be degraded naturally by self-purification ability in the ecosystem [3]. Therefore, it is crucial to seek a suitable method to treat tetracycline in water. Lots of physical, biological, and chemical technologies have been explored to remove tetracycline from wastewater, including adsorption, anaerobic anoxia aerobic (AAO) process, and advanced oxidation processes (AOP) [4–7], *etc*. In AOP, electrocatalytic degradation of tetracycline has broad application prospects due to its advantages such as high efficiency, green chemistry, convenient operation and so on [8]. Cai et al. [9] fabricated a stable boron and cobalt co-doped TiO_2 nanotube anode material for the electrocatalytic degradation of tetracycline with enhanced electrode lifetime over 100 times compared with undoped samples.

Recently, the application of an external magnetic field is considered a potential way to improve the electrocatalytic performance [10]. Sun et al. [11] found that enhancing the spin state of cobalt cation in spinel ($ZnCo_2O_4$) by magnetic field could propagate the spin channel to strengthen the spin-selective charge transfer in the oxygen evolution reaction (OER) process and produce better active sites for the adsorption of intermediates. Pan et al. [12] reported that the catalytic activity of tin nanoparticles for electrocatalytic reduction of CO_2 to formate/formic acid was remarkably improved by magnetic field. Nevertheless, there are no reports on the magnetic field enhanced electrocatalytic degradation of antibiotics yet.

Phthalonitrile resin, as a thermosetting resin with excellent thermal and anti-oxidative stability, flame retardancy, and high carbon yield, is an outstanding precursor for constructing the carbon material [13]. Weng et al. [14] annealed the mixture of 1,3-bis(3,4-dicyanophenoxy) benzene (phthalonitrile precursor) with urea and KOH to obtain the porous carbon materials with high specific surface area (2194 $m^2\ g^{-1}$). Besides, Gao et al. [15] successfully prepared a phthalonitrile resin by

* Corresponding authors.
E-mail addresses: zhouheng@iccas.ac.cn (H. Zhou), hongbogu2014@tongji.edu.cn (H. Gu).

https://doi.org/10.1016/j.apcatb.2023.123225
Received 8 June 2023; Received in revised form 22 August 2023; Accepted 24 August 2023
Available online 25 August 2023

utilizing polyaniline (PANI) as catalyst and 1,3-bis(3,4-dicyanophenoxy)benzene (MPN) as monomer, which exhibited a high carbon yield up to 24.7 % at 850 ℃. These reports provide the theoretical basis for the preparation of porous carbonized phthalonitrile resin with KOH as pore-forming agent and PANI as catalyst.

Based on the mentioned above, in this work, aiming to explore the magnetic field effect on the electrocatalytic degradation of tetracycline, a novel magnetic porous carbonized phthalonitrile resin was designed by annealing the mixture of 1,3-bis(3,4-dicyanophenoxy)benzene (MPN, a kind of PN resin monomer), polyaniline coated barium ferrite, and KOH. The optimal preparation condition of samples and the effect of magnetic field strength on the electrocatalytic degradation of tetracycline were systematically studied. Parameters like bias voltages, pH values, and initial concentrations of tetracycline, *etc*. were also comprehensively investigated at an external magnetic field of 200 mT. The possible magnetic field promoted electrocatalytic degradation mechanism and degradation pathways of tetracycline were proposed. This work opens a new direction for the application of the magnetic field in the electrocatalytic degradation of antibiotics in contaminated water.

2. Materials and methods

2.1. Materials

Tetracycline hydrochloride ($C_{22}H_{24}N_2O_8$·HCl, 97.5 %), aniline (C_6H_7N, 99.5 %), *p*-toluenesulfonic acid (PTSA, $C_7H_8O_3S$, 99 %), anhydrous ethanol (C_2H_5OH) and ammonia (NH_3·H_2O, 25–28 wt%) were purchased from Shanghai Macklin Biochemical Co., Ltd. Ferric nitrate ($Fe(NO_3)_3$·9 H_2O, 98.5 %), barium nitrate ($Ba(NO_3)_2$, 99.5 %), citric acid (CH_3COOH, 99.5 %) and potassium hydroxide (KOH, 85 %) were supplied by Sinopharm Chemical Reagent Co., Ltd. Ammonium persulfate (APS, $(NH_4)_2S_2O_8$, 98.5 %), resorcinol ($C_6H_6O_2$, 99 %) and 4-aminophenol (C_6H_7NO, 99.5 %) were provided by Aladdin Reagent Company (China). 4-nitrophthalonitrile ($C_8H_3N_3O_2$, 98.0 %) was offered by Alpha Chemical Co., Ltd (Shijiazhuang, China). All chemicals were used without further purification after received.

2.2. Preparation of magnetic porous carbonized phthalonitrile resin

Firstly, ferric nitrate (19.3926 g) and barium nitrate (1.0454 g) were dissolved in 10 mL of deionized water in water bath at 30 ℃. Next, citric acid (9.9926 g) was added into the solution under magnetic stirring for 1 h. Secondly, the pH of solution was adjusted to about 7 by dripping ammonia. Then, the temperature of water bath was raised to 80 ℃. After becoming sol-gel, it was heated to about 200 ℃ and subsequently ignited to obtain barium ferrite precursor. After that, the barium ferrite precursor was ground in a mortar and pestle and placed in a tubular furnace (GSL-1100X-S, Kejing Co. Ltd., Hefei, China) to calcinate at 900 ℃ for 10 h to acquire the barium ferrite nanoparticles. Afterwards, 0.4198 g of barium ferrite nanoparticles (*i.e.,* 40 wt% of the final product), 2.0509 g of APS and 2.8524 g of PTSA were added into 100 mL of deionized water under sonication and mechanical stirring in the ice-water bath for 1 h. Then, 1.64 mL of aniline was slowly added into the above mixture. After 2 h of *in-situ* polymerization of aniline, the product was vacuum filtered and washed by water and ethanol for three times to remove the excess oligomers and salts. The product was freeze-dried for 12 h, labeled as 40BPANI. Similarly, 60BPANI, 20BPANI and pure PANI were also respectively prepared by the same procedure. Additionally, the synthesis of MPN ($C_{22}H_{10}N_4O_2$, chemical structure is shown in Fig. S1) was conducted according to our previous report [16] and the detailed procedure was described in Supplementary material.

Finally, 1.0 g of MPN (monomer), 0.5 g of 40BPANI (catalyst), and 1.0 g of KOH (pore-forming agent) were blended by grinding. Thereafter, the mixture was placed in the tubular with the annealing sequences of 300 ℃ for 1 h and 850 ℃ for 1 h to acquire the carbonized 40BPANI/MPN resin, labeled as 40BPM850. The samples including 60BPM850, 20BPM850, PM850 (pure PANI as catalyst), 40BPM650, 40BPM700, 40BPM750, 40BPM800, 40BPM850, and 40BPM900 were also respectively synthesized in the same way for comparison.

2.3. Characterizations

X-ray diffraction (XRD) analysis was applied to characterize the crystalline structures of samples by a Bruker AXS D8 Advance X-ray diffractometer with a general area detector diffraction system (GADDS) and data were collected in a range of 10–80°. X-ray photoelectron spectroscopy (XPS) analysis was conducted with a Thermo escalab 250Xi spectrometer with Al Kα ($h\nu = 1486.6$ eV) radiation as the excitation source at a power of 150 W. The microstructures of samples were recorded on a high-resolution transmission electron microscopy (HRTEM, Tecnai G2 F20, FEI Company) and a field emission scanning electron microscope (SEM, Hitachi S-4800 system). Brunauer-Emmett-Teller (BET) adsorption and desorption isotherms were gained from a surface area analyser (TriStar 3020, Micromeritics Instrument Ltd.). The thermogravimetric analysis (TGA) was carried out within the temperature range from 30 to 800 ℃ in the air conditions with a heating rate of 20 ℃ min^{-1} by a TGA55 (TA company). Raman spectra of samples were collected in the range of 4000–500 cm^{-1} on the Raman spectrometer (Invia, Renishaw Inc.). The magnetic properties were measured on a Physical Properties Measurement System (PPMS, Quantum Design) at room temperature. The tetracycline solutions after electrocatalytic degradation by samples were scanned on inductively coupled plasma optical emission spectrometer (ICP-OES, PE Optima 8300, PerkinElmer Inc.) to affirm that no metal was leaked out after treatment.

2.4. Electrode preparation and electrocatalytic degradation evaluation of tetracycline

To obtain a magnetic porous carbonized phthalonitrile resin electrode for electrocatalytic degradation of tetracycline, around 1.0 mg of as-prepared sample was weighed by a microbalance (SQP, Sartorius) and uniformly adhered to a conductive tape (Ted Pella, Inc.) with the diameter of 12 mm which was attached to a Toray carbon paper (1.5 cm × 3 cm) under pressure. The different tetracycline concentrations were obtained by diluting 1.0 g L^{-1} of tetracycline stock solution with deionized water. The tetracycline concentration mainly used in this work was 20 mg L^{-1}. A magnetic porous carbonized phthalonitrile electrode (as the working electrode and anode), a saturated calomel electrode (SCE, as reference electrode, type 232, Tianjin Aida Hengsheng Technology Co., Ltd) and a platinum electrode (as counter electrode, Φ0.5 × 37–25 mm, Tianjin Aida Hengsheng Technology Co., Ltd) were connected to the electrochemical workstation (CHI760E, Shanghai Chenhua Instrument Co., Ltd). 20 mL of tetracycline solution (20 mg L^{-1}) was added into the electrolytic cell. The electrocatalytic degradation was carried out in the time-current mode at room temperature for 2 h. The tetracycline concentrations in the solutions for all the experiments were measured by high-performance liquid chromatography (HPLC, UltiMate3000, Thermo Fisher Scientific Inc.) with the rate of 0.800 mL min^{-1}, the column temperature of 30 °C, and the mobile phase of 25 % methanol and 75 % water at the wavelength of 356.5 nm. The reported value for each sample was the average of three measurements with a standard deviation within ± 2.0%. The tetracycline degradation percentage (DP%) was calculated by Eq. (S1).

2.4.1. Optimal conditions for the synthesis of magnetic porous carbonized phthalonitrile

In order to figure out the optimal conditions for preparing the magnetic porous carbonized phthalonitrile resin, different parameters including loading levels of barium ferrite like 20BPANI, 40BPANI, 60BPANI and pure PANI, and annealing temperature such as 650, 700, 750, 800, 850 and 900 ℃ were applied to fabricate the magnetic porous carbonized phthalonitrile. The electrodes made from these magnetic

porous carbonized phthalonitrile resins were separately employed in the electrocatalytic degradation of 20 mL tetracycline solutions over the same treatment period of 2 h at room temperature to assess their electrocatalytic degradation capabilities to tetracycline. Later, the solutions were taken out for HPLC measurements.

2.4.2. Effect of magnetic field strength

In the time-current mode, different magnetic field strengths including 0, 100, 150, and 200 mT were employed by external electromagnet (Hunan Forever Elegance Technology Co., Ltd) to explore the electrocatalytic degradation performance of 20 mL tetracycline solution with the initial concentration of 20 mg L^{-1} and 0.1 mol L^{-1} of Na_2SO_4 as supporting electrolyte at pH of 5.0 for 2 h by 20BPM850, 40BPM850, and 60BPM850 at the bias voltage of 1.0 V (*vs*. SCE), respectively. Then, the solutions were used for HPLC measurement.

2.4.3. Effect of bias voltage

With the purpose of figuring out the effects of different bias voltages on the electrocatalytic degradation of 20 mL tetracycline solution at pH of 5.0 with an initial concentration of 20 mg L^{-1} by 40BPM850, a series of bias voltages (1.2, 1.0, 0.8, and 0.6 V, respectively) were applied for the electrocatalytic degradation under the magnetic field strength of 200 mT.

2.4.4. Effect of pH value

The effect of pH value on the electrocatalytic degradation of tetracycline was investigated by selecting pH values of 3.0, 5.0, 7.0, 9.0 and 11.0, respectively, in 20 mL of tetracycline solution with an initial concentration of 20 mg L^{-1} and 0.1 mol L^{-1} of Na_2SO_4 as supporting electrolyte for 2 h at the bias voltage of 1.0 V (*vs*. SCE) by 40BPM850 under the magnetic field strength of 200 mT. The pH value of tetracycline solutions was adjusted by NaOH (1.0 mol L^{-1}) and H_2SO_4 (1.0 mol L^{-1}) with a pH meter (PHS-3E).

2.4.5. Effect of initial tetracycline concentration

The initial tetracycline concentration effect on the electrocatalytic degradation of tetracycline by 40 BPM850 was studied by treating 20 mL of tetracycline solutions with 0.1 mol L^{-1} of Na_2SO_4 as supporting electrolyte at pH of 5.0 with an initial tetracycline concentration ranging from 10 to 40 mg L^{-1} for 2 h at the bias voltage of 1.0 V (*vs*. SCE) under the magnetic field strength of 200 mT.

2.4.6. Kinetic study and power consumption analysis

In the kinetic study, the electrocatalytic degradation of tetracycline was performed in 20 mL of tetracycline solution with an initial tetracycline concentration of 20 mg L^{-1} and 0.1 mol L^{-1} of Na_2SO_4 as supporting electrolyte at pH of 5.0 for different treatment time from 0.5 to 2 h by 40BPM850 under the magnetic field strength of 200 mT. Power consumption and Faraday efficiency were also calculated to measure the electrocatalytic degradation efficiency of 40BPM850 to tetracycline.

2.4.7. Recyclability of magnetic porous carbonized phthalonitrile resin modified electrode

The 40BPM850 modified electrode was exploited to carry out the electrocatalytic degradation in 20 mL of tetracycline solution with an initial tetracycline concentration of 10 mg L^{-1} and 0.1 mol L^{-1} of Na_2SO_4 as supporting electrolyte for 2 h at pH of 5.0 under the magnetic field strength of 200 mT. After degradation, the solution was sampled for the residual tetracycline concentration determination by HPLC. Then, the above procedures were repeated with the used 40BPM850 modified electrode for further electrocatalytic degradation. The retention was run for 10 times to explore the stability and reusability of 40BPM850.

2.4.8. Electrocatalytic degradation mechanism and pathways of tetracycline by magnetic porous carbonized phthalonitrile resin with and without magnetic field

For exploration of electrocatalytic degradation mechanism of tetracycline, the 10 mg L^{-1} of tetracycline solutions before and after treatment were tested by HPLC and the total organic carbon (TOC) (Analytik Multi N/C 3100, Analytik Jena Inc.). Besides, for comparison, 20 mL of tetracycline solution was electrocatalytically degraded for 4 h by 40BPM850 modified electrode with and without magnetic field. The initial concentration of tetracycline was 100 mg L^{-1} in case the concentrations of degraded products were too low to be detected by the high-performance liquid chromatography and quadrupole time of flight mass spectrometry (HPLC-MS, Agilent 1290II-6460) in a positive ion mode.

3. Results and discussion

3.1. Structure characterizations of magnetic porous carbonized phthalonitrile resins

With the aim to figure out the structure of as-prepared magnetic porous carbonized phthalonitrile resins, the XRD, XPS, SEM, HRTEM, BET, TGA, and Raman characterizations have been performed. The XRD patterns of 40BPM850, 20BPM850, and 60BMP850 are shown in Fig. 1 (A) and Fig. S3, respectively. It is noted that the strong diffraction peaks of 60BPM850 located at 44.7 and 65.0° are respectively correlated with (1 1 0), and (2 0 0) crystallographic planes of the body-centered cubic phase of iron (JCPDS No. 06–0696) [17], Fig. S3. Meanwhile, the diffraction peaks of 20BPM850 at 26.4, 42.3, 44.5, 59.6 and 76.8° could be evidently observed, which are accordingly associated with (0 0 2), (2 0 0), (2 0 1), (2 0 3), (3 1 0) crystallographic planes of FeC (JCPDS No. 03–0411) [18]. There are also clear peaks at around 44.5 and 65.0° corresponding to the body-centered cubic phase of iron in XRD pattern of 20BPM850, Fig. S3. Compared with 20BPM850 and 60BPM850, 40BPM850 exhibits the relatively weak characteristic diffraction peaks, Fig. 1(A), implying that the magnetic porous carbonized phthalonitrile resin could form the different crystalline phases with different loadings of barium ferrite.

The chemical element compositions and chemical valence states of 40BPM850 are analysed by XPS. Generally, the XPS wide-scan survey spectrum of 40BPM850 displays the presence of Ba 3d, Fe 2p, O 1s, C 1s and S 2p peaks at ~781, ~711 ~531, ~284, and ~164 eV, respectively, Fig. S4, and the corresponding element contents are laid out in Table S1. It is found that the Ba element with low element content is doped in the 40BPM850. The C 1s high-resolution XPS spectrum of 40BPM850 in Fig. 1(B) could be deconvoluted into two peaks at 284.5 and 285.9 eV, assigned to C-C and C-O-Fe bonds, respectively [19]. Markedly, the C-O-Fe bond is closely related to the interaction between iron and carbon system. In the Fe 2p high-resolution XPS spectrum of 40BPM850, Fig. 1(C), the peaks located at around 710 and 725 eV belong to Fe $2p_{3/2}$ and Fe $2p_{1/2}$, in which peaks at 714.0 and 726.3 eV are ascribed to Fe (III) and peaks at 711.2 and 724.5 eV are attributed to Fe(II), accordingly [20,21]. The oxidation state of Fe, *i.e.,* Fe(III) and Fe(II), may come from the oxidation of air on the material surface. However, the obvious characteristic of oxidation state for Fe does not exist in the XRD pattern of 40BPM850, which may be due to the low content of oxidation components in 40BPM850 [22].

The SEM image of 40BPM850 is illustrated in Fig. 1(D), in which the pore structures with diameter of approximate 300–600 nm are obviously observed. During the annealing process, KOH plays a decisive role in promoting the formation of pore structures as a pore-forming agent. Further analysis of the detailed morphology and microstructures for 40BPM850 could be conducted through the TEM images, Fig. 1(E) and (F). The result depicted in Fig. 1(E) indicates that the skeleton of 40BPM850 is composed of amorphous carbon with crystalline nanoparticles distributed on the surface and inside of the carbon system.

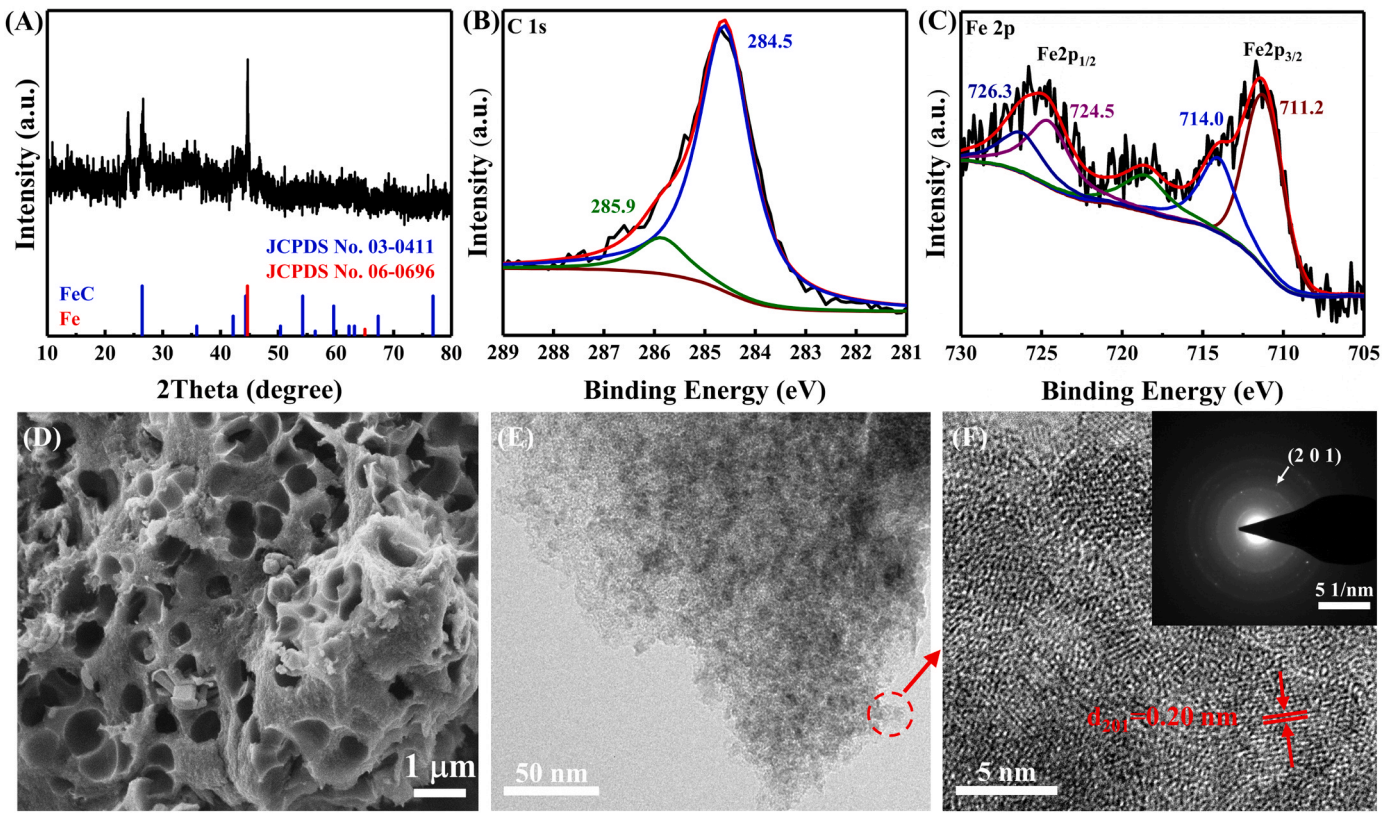

Fig. 1. . (A) XRD pattern of 40BPM850; high-resolution XPS spectra of 40BPM850 for (B) C 1 s; (C) Fe 2p; (D) SEM image; (E) TEM image; and (F) high-resolution TEM (HRTEM) image (main) and selected area electron diffraction (SAED) of 40BPM850 (inset).

From the high-resolution TEM (HRTEM) image, Fig. 1(F), a typical lattice fringe spacing of 0.20 nm is noticed, which corresponds to the (2 0 1) crystallographic plane of FeC. The selected area electron diffraction (SAED) that is inset in Fig. 1(F) displays the diffraction rings, in which the diffraction ring of (2 0 1) crystallographic plane is easily measured. These results are consistent with the XRD analysis above.

The pore properties of magnetic porous carbonized phthalonitrile resins are investigated by N_2 adsorption-desorption isotherms. As shown in Fig. 2(A), the pore size of 40BPM850 is mainly distributed in the range of 2–5 nm. Importantly, the BET surface area of 60BPM850, 40BPM850, 20BPM850 and PM850 is revealed in Fig. 2(B), which reaches the value of 198.9, 1299.1, 1498.1 and 1814.8 $m^2\ g^{-1}$, accordingly. It is worth noting that PM850, as a porous carbon material in SEM image of Fig. S5(A), has the highest BET surface area among these samples. However, as the loading level of barium ferrite increases, the BET surface area of magnetic porous carbonized phthalonitrile resins is significantly decreased, especially for 60BPM850. Meantime, the effect of annealing temperature on the pore properties of these magnetic porous carbonized phthalonitrile resins has also been studied, as demonstrated in Fig. 2(C). It is found that from 650 to 850 °C, the BET surface area of 40BPM650, 40BPM700, 40BPM750, 40BPM800, and 40BPM850 manifests an upward trend, but this value decreases when the annealing temperature approaches 900 °C. This phenomenon might be attributed to the destroy of the material pore framework under high temperature treatment. The BET surface area data of magnetic porous carbonized phthalonitrile resins is listed in Table S3.

The TGA curves of magnetic porous carbonized phthalonitrile resins are depicted in the Fig. S9(B). It is noted that the residual weight of PM850, 20BPM850, 40BPM850 and 60BPM850 is 1.57 %, 20.28 %, 39.54 % and 95.79 %, respectively, recommending that the carbon content in the magnetic porous carbonized phthalonitrile resins decreases with raising the barium ferrite loading levels. The magnetic

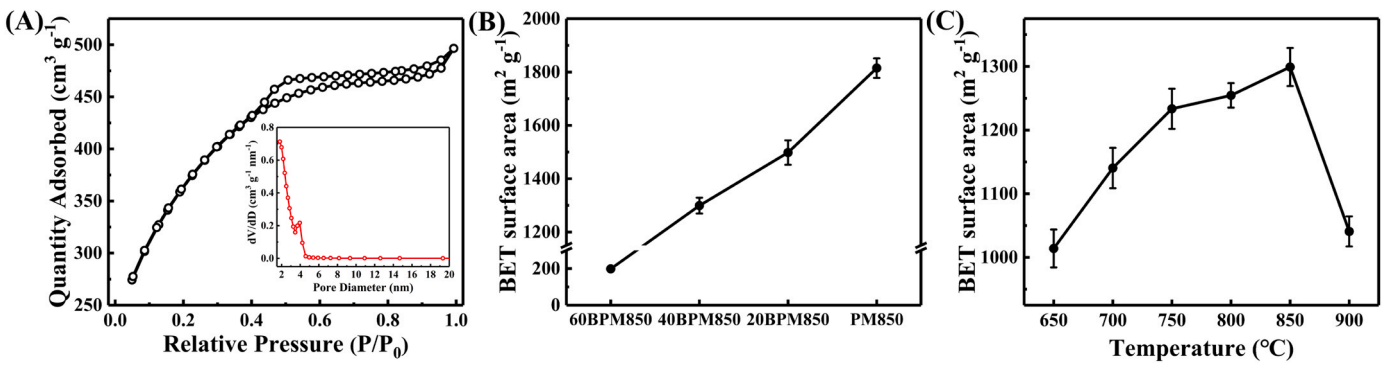

Fig. 2. . (A) Nitrogen adsorption-desorption isotherm and pore size distribution of 40BPM850; BET surface areas of (B) 60BPM850, 40BPM850, 20BPM850 and PM850; (C) 40BPMs annealed at the temperatures from 650 to 900 °C.

properties of samples have also been studied and illustrated in Fig. S10. The saturation magnetization (M_s) values of 20BPM850, 40BPM850 and 60BPM850 are measured to be 7.5, 12.5 and 69.7 emu g^{-1} and the coercivity (H_c) values are found to be 83, 84 and 102 Oe, accordingly, lower than 200 Oe, exhibiting a superparamagnetic property [23]. Besides, the Raman spectrums of magnetic porous carbonized phthalonitrile resins are seen in Fig. S11. The peaks for D-band and G-band have been deconvoluted by fitting to gain the full width at half maximum (FWHM) in D-band, since the FWHM in D-band can reflect the degree of defects in the carbon system [24,25]. With increasing loading levels of barium ferrite in the catalyst, the FWHM in D-band decreases from 230.5 cm^{-1} (PM850) to 190.0 cm^{-1} (60BPM850). As the barium ferrite loading level is grown, the degree of defects in the carbon system for samples slightly decreases.

In summary, based on the characterization results above, the magnetic porous carbonized phthalonitrile resins with high specific surface areas have been successfully synthesized and their chemical structures can be recognized as Ba-doped Fe@FeC/carbon material. According to the literature, these kinds of materials probably possess the excellent electrocatalytic degradation performance to antibiotics comparable to noble metals [26,27].

3.2. Optimal condition for preparation of magnetic porous carbonized phthalonitrile resins and magnetic field strength effect

The exploration of optimal preparation condition for the magnetic porous carbonized phthalonitrile resins is necessary for attaining the best electrocatalytic degradation performance of tetracycline. Firstly, the magnetic porous carbonized phthalonitrile resins fabricated under different annealing temperatures from 650 to 900 ℃ separately undergo the tetracycline degradation experiment at a bias voltage of 1.0 V (*vs.* SCE) in a 20 mg L^{-1} of tetracycline solution for 2 h. As exhibited in Fig. 3(A), the results evince that the tetracycline DP% discloses an increasing tendency from 40BPM650 to 40BPM850, whose values are 48.91 %, 52.50 %, 55.45 %, 59.58 % and 63.25 %, respectively. However, when the annealing temperature further increases to 900 ℃, tetracycline DP% obviously declines to 58.61 %. This phenomenon might be closely related to the destruction of pore structures in 40BPM900 at high annealing temperature, which is consistent with the BET results. This connotes the importance of porous structure in the sample for the electrocatalytic degradation of tetracycline.

Then, the impact of barium ferrite loading level on the tetracycline degradation has been studied in a 20 mg L^{-1} of tetracycline solution for 2 h at the bias voltage of 1.0 V (*vs.* SCE), as emphasized in Fig. 3(B)-(D) without applying the external magnetic field. Tetracycline DP% by 20BPM850, 40BPM850 and 60BPM850 is dropped sequentially with values of 69.99 %, 63.25 % and 56.22%, respectively. Interestingly, the tetracycline DP% by PM850 under this condition reaches 73.27 %, Table S5. This signifies that the highest electrocatalytic degradation performance is achieved in the PM850 sample without magnetic field, in which the barium ferrite loading level is 0.

In a word, the optimal condition for manufacturing the samples with the highest electrocatalytic degradation performance of tetracycline is the annealing temperature of 850 °C and the barium ferrite loading level

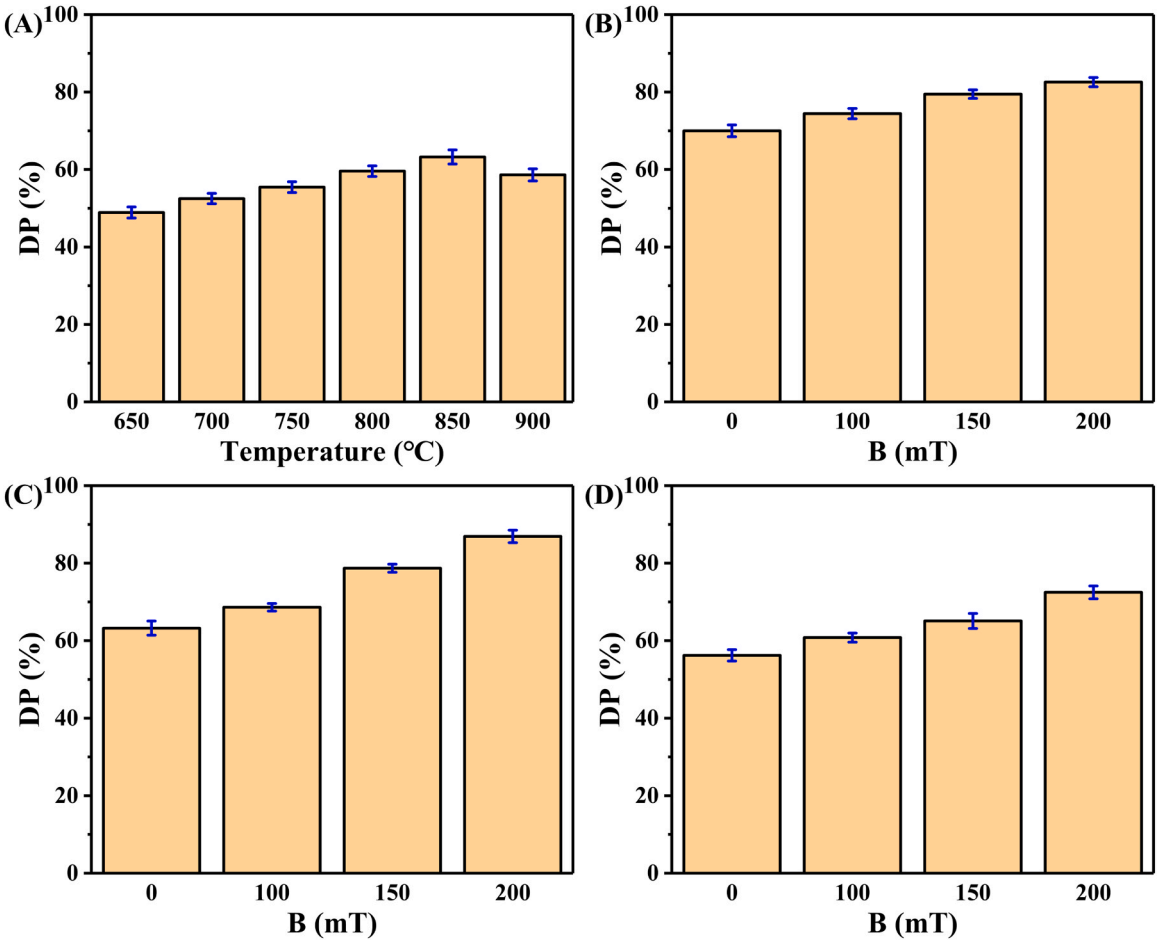

Fig. 3. . (A) DP% in the tetracycline solutions (20 mL, 20 mg L^{-1}, pH of 5.0, with 0.1 M Na_2SO_4) at a bias voltage of 1.0 V (*vs.* SCE) without magnetic field by 40BPMs annealed at the temperatures from 650 to 900 ℃; DP% in the tetracycline solutions (20 mL, 20 mg L^{-1}, pH of 5.0, with 0.1 M Na_2SO_4) at a bias voltage of 1.0 V (*vs.* SCE) with different external magnetic field strength by (B) 20BPM850; (C) 40BPM850; (D) 60BPM850.

is 0 (*i.e.*, PM850) without magnetic field. Unfortunately, the magnetic field has no significant effect on the electrocatalytic degradation performance to tetracycline of PM850, Table S5. In the following, the magnetic field effect on the electrocatalytic degradation of tetracycline by 20BPM850, 40BPM850, and 60BPM850 is assessed.

The magnetic field strength effect on the electrocatalytic degradation of tetracycline by 20BPM850, 40BPM850, and 60BPM850 is examined and the results are arranged in Fig. 3(B)-(D). Surprisingly, it is noticed that the tetracycline DP% increases with increasing magnetic field strength from 0 to 200 mT for 20BPM850, 40BPM850 and 60BPM850, Table S5. Under the magnetic field of 200 mT, the tetracycline DP% by 20BPM850, 40BPM850 and 60BPM850 is 82.57 %, 86.92% and 72.47%, accordingly, which increases up to 17.97%, 37.42% and 28.90% relative to those without magnetic field (69.99 %, 63.25 % and 56.22%, respectively). This intimates that the magnetic field has more effect to the electrocatalytic degradation performance of 40BPM850 compared with 20BPM850 and 60BPM850. As a result, the 40BPM850 is considered for the further studying the electrocatalytic degradation parameters of tetracycline such as bias voltages, pH values, initial tetracycline concentrations, and degradation time, *etc*.

3.3. Parameters effect on the tetracycline degradation

In the following, the effect of bias voltages, pH values, initial concentrations of tetracycline, degradation time, and recyclability on the electrocatalytic degradation of tetracycline by 40BPM850 under an external magnetic field of 200 mT have been performed. Firstly, in a 20 mg L^{-1} of tetracycline solution, the tetracycline degradation has been conducted at different bias voltages (0.6–1.2 V *vs*. SCE) for 2 h under an external magnetic field of 200 mT and the obtained results are shown in Fig. 4(A). When the bias voltage (*vs*. SCE) is 0.6 V, the tetracycline DP% is 45.54 %. As the bias voltage increases to 1.0 V, the DP% increases to 86.92 %. With continuously increasing the bias voltage to 1.2 V, the tetracycline DP% obviously decreases to 63.53 %. Since the bias voltage of anode at 1.2 V is very close to the theoretical splitting voltage of water at 1.23 V, many bubbles are generated on the anode surface, denoting the occurrence of oxygen evolution reaction (OER) [28]. It is reported that the external magnetic field is beneficial for promoting the OER, so that the gas evolution side reactions may hinder the degradation of tetracycline and even affect the stability of the electrode [29]. Consequently, the following tests have been carried out at the bias voltage of 1.0 V (*vs*. SCE).

Secondly, the effect of pH values on tetracycline degradation has been studied with the pH values varied from 3.0 to 11.0 in a 20 mg L^{-1} of tetracycline solution for 2 h at the bias voltage of 1.0 V (*vs*. SCE) under an external magnetic field of 200 mT, as displayed in Fig. 4(B). It's found that the pH value has a vital impact on the tetracycline DP% by 40BPM850. Clearly, the optimal pH value for the electrocatalytic degradation of tetracycline is lower than 5 in this system. Generally, there are several ionizable functional groups in the tetracycline molecule and their existence depends on the pH values [30]. At the low pH value, amino groups can be protonated, and the oxidation between molecules and hydroxyl radical is more likely to occur. In contrast, in the alkaline environment, tricarbonylamide and phenolic diketones would be deprotonated, resulting in the blocked reaction. The tetracycline DP % is 88.26 %, 86.92 %, 77.20 %, 75.15 % and 71.54 % in the solution with the pH values of 3.0, 5.0, 7.0, 9.0 and 11.0, respectively. Even though the system with strong acidity could improve the tetracycline DP %, the corrosion of electrodes is hardly to be avoided [31]. From the perspective of extending the service life for electrode, the ICP-OES

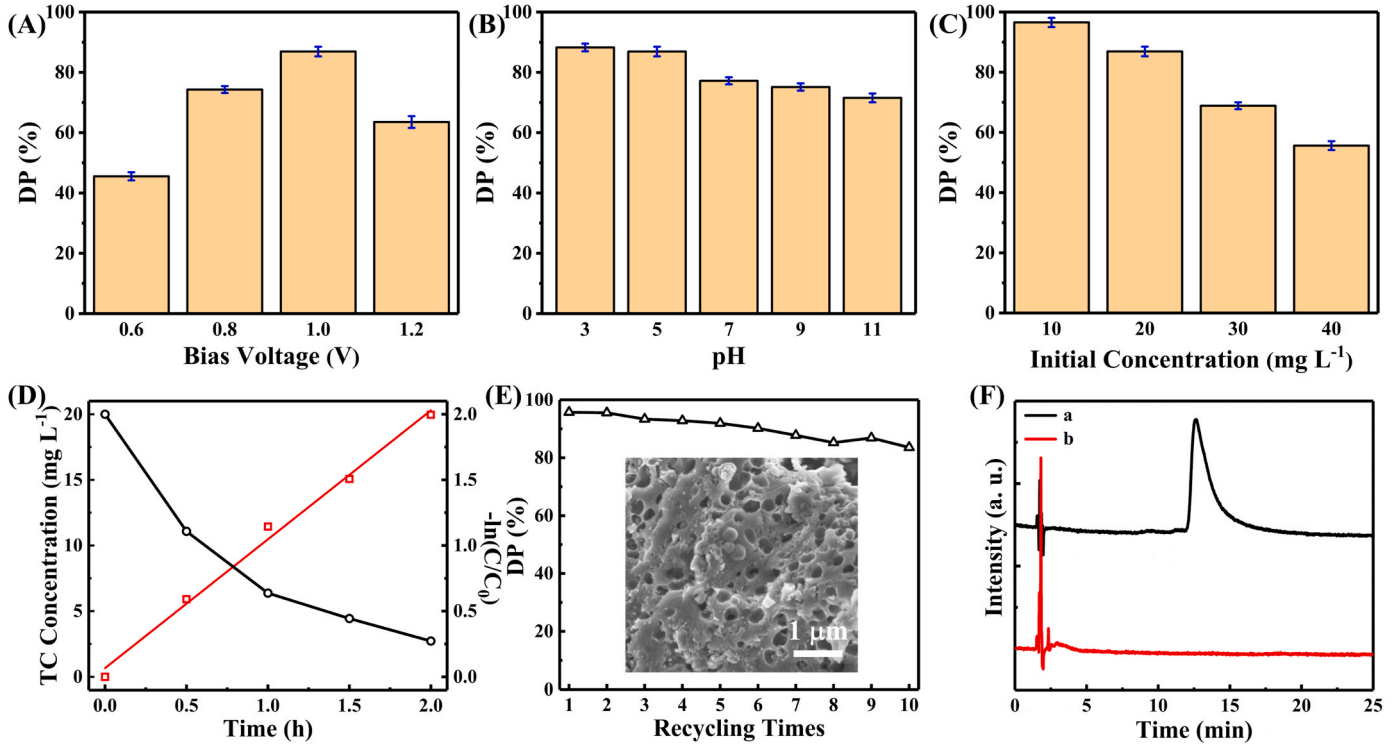

Fig. 4. . (A) DP% in the tetracycline solutions (20 mL, 20 mg L^{-1}, pH of 5.0, with 0.1 M Na_2SO_4) under an external magnetic field of 200 mT at different bias voltages by 40BPM850; (B) DP% in the tetracycline solutions (20 mL, 20 mg L^{-1}, pH varied from 3.0 to 11.0, with 0.1 M Na_2SO_4) under 200 mT at 1.0 V by 40BPM850; (C) DP% in the tetracycline solutions (20 mL, initial concentration varied from 10 to 40 mg L^{-1}, pH of 5.0, with 0.1 M Na_2SO_4) under 200 mT at 1.0 V by 40BPM850; (D) tetracycline concentration after treatment of 20 mL tetracycline solution (20 mg L^{-1}, pH of 5.0, with 0.1 M Na_2SO_4) under 200 mT at 1.0 V with different time at room temperature (black line) and corresponding kinetic plot (red line); (E) DP% of tetracycline solutions (20 mL, 10 mg L^{-1}, pH of 5.0, with 0.1 M Na_2SO_4) at 1.0 V (*vs*. SCE) for 2 h catalyzed by recycled 40BPM850 at room temperature (main) and the SEM image of 40BPM850 after recycled for 10 times (inset); (F) HPLC results at the detection band of 365.5 nm for (a) 10 mg L^{-1} of tetracycline solution and (b) tetracycline solution (20 mL, 10 mg L^{-1}) treated by 40BPM850 for 24 h at the bias voltage of 1.0 V (*vs*. SCE) under a magnetic field of 200 mT.

experiments have confirmed that the optimal pH value of tetracycline solution for the electrocatalytic degradation by 40BPM850 is 5.0, since there are no obvious metal ions existed in the solution after the electrocatalytic degradation process, as shown in Table S6. In addition, the concentrations of Fe and Ba elements in treated solutions with values of 0.3 and 0.7 mg L^{-1}, respectively, are all lower than the standard limits from the *Environmental quality standards for surface water of China* (GB 3838–2002).

Then, the degradation results of solutions with different initial tetracycline concentrations for 2 h with a bias voltage of 1.0 V (*vs*. SCE) under an external magnetic field of 200 mT are displayed in Fig. 4(C). It is worth mentioning that the tetracycline DP% with initial concentrations of 10, 20, 30, and 40 mg L^{-1} is 96.54%, 86.92%, 68.86% and 55.60%, respectively. Commonly, the concentration of tetracycline wastewater is at the level of μg L^{-1} and the diffusion velocity of tetracycline to the electrode, rather than the degradation reaction rate, is the rate-determining step of the system [32]. Thanks to the outstanding adsorption capacity of the pore structures in 40BPM850, the low concentration of tetracycline in the solution can be quickly accumulated on the surface of electrode, ensuring the effective electrocatalytic process and higher tetracycline DP%.

Next, at the bias voltage of 1.0 V (*vs*. SCE) under a magnetic field of 200 mT, 20 mL of tetracycline solution (20 mg L^{-1}) is treated for investigating the kinetics of tetracycline degradation by 40BPM850 modified electrode, as depicted in Fig. 4(D). The tetracycline concentration (C)~treatment time (t) plot reveals that the C rapidly decreases at the beginning and then slowly decreases with increasing t, which conforms to the characteristics of pseudo-first-order kinetic model. Usually, the pseudo-first-order reaction kinetics is described as Eq. (S2). The fitted result is shown in Fig. 4(D), in which the plot of $-\ln[C/C_0]$~t is well linearly fitted with the pseudo-first-order kinetic model (R^2 =0.9930). At the bias voltage of 1.0 V (*vs*. SCE) with current lower than 1 mA, the degradation rate constant k is calculated from the intercept ($1/k$) of the $-\ln[C/C_0]$~t linear plot with a value of 0.9815 h^{-1}.

Finally, the recyclability of 40BPM850 modified electrode is researched by repeatedly using the same electrode to electrostatically degrade the tetracycline solution for 2 h under an external magnetic field of 200 mT at a voltage of 1.0 V (*vs*. SCE). The tetracycline DP% at the first and tenth electrocatalytic degradations is 95.15 % and 83.55 %, respectively, demonstrating that the change of tetracycline DP% is relatively small after 10 recycling times, as laid out in Fig. 4(E). The SEM image of 40BPM850 modified electrode after 10 recycling times is recorded in the inset of Fig. 4(E). Compared with the SEM image in Fig. 1 (D), there is no obvious change after 10 recycling times, illustrating the good stability and reusability of 40BPM850 modified electrode.

3.4. Possible magnetic field enhanced electrocatalytic degradation mechanism and degradation pathways exploration

The possible magnetic field enhanced electrocatalytic degradation mechanism and degradation pathways of tetracycline by magnetic porous carbon phthalonitrile resins have been judged successively. Firstly, the initial reaction on the anode (noted as M) corresponds to the formation of physically adsorbed hydroxyl radical (noted as M(OH·)) due to the oxidation of water in Eq. (1).

$$M + H_2O \rightarrow M(OH\cdot) + H^+ + e^- \quad (1)$$

Normally, the complete mineralization of organic pollutants is taken place on anodes that can physically accumulate OH·(*i.e.*, M(OH·)) but do not further form the chemical bond, and such anodes are classified as non-active anode [33]. Then, the oxygen from M(OH·) also has the possibility to enter the lattice of the anode material to form the chemically adsorbed lattice oxygen (MO species) as Eq. (2).

$$M(OH\cdot) \rightarrow MO + H^+ + e^- \quad (2)$$

Such anodes are recorded as active anode and the selective oxidation occurs on such anodes that can form the lattice oxygen species (*i.e.,* MO species).

It is reported that the isopropanol can be utilized as a quencher of hydroxyl radical to monitor whether there is a reaction between tetracycline and hydroxyl radical [34]. After adding isopropanol to the tetracycline solution to reach a concentration of 1 mol L^{-1}, the tetracycline DP% significantly decreases from 86.92 % to 64.59 % by 40BPM850, which proves the existence of the process in Eq. (1). Additionally, it is recognized that there is no peak of tetracycline in the treated solution (20 mL, 10 mg L^{-1}) at the detection band of 365.5 nm (retention time at ~12.5 min), Fig. 4(F), and the related species of tetracycline during degradation process also not observed in other detection bands including 276, 230 and 210 nm, Fig. S13. Nevertheless, the TOC result of this tetracycline solution is about 79.7 % after treatment, representing that there are still small organic molecules left and they could not be detected in HPLC-MS. This means the occurrence of selective oxidation for the electrocatalytic degradation of tetracycline by 40BPM850, indicating the characteristic of active anode. Generally, for the active anode, MO species act the main role in the electrocatalytic degradation of antibiotics [33].

In line with the literature, it is reported that there are two types of spin configurations of MO containing M-O·and M=O [35]. The spin configuration of M-O·and M=O in the magnetic porous carbon phthalonitrile resins can be represented as Fig. 5(A)-(a) and (b), respectively. The spin alignment of metal sites under the action of an external magnetic field can promote spin polarization of oxygen ligand radicals, so that two electrons are arranged in spin parallel in the $d\pi$ and $p\pi$ orbitals and an unpaired p electron remains on oxygen, *i.e.*, M-O·, Fig. 5(A)-(a) [36]. Nonetheless, in the absence of an external magnetic field, oxygen ligands tend to form π bonds with metal sites, where there are paired electrons with opposite spin, *i.e.,* M=O, 5(A)-(b). As described in Fig. 5 (B)-(a), the dominant species M-O· under the spin alignment effect of an external magnetic field can meet the conditions for spin-selective electron removal when the reaction between tetracycline molecule (R) and M-O· occurs. This expresses a relatively low energy barrier situation since the electron removal in a specific spin direction can be promoted by a ferromagnetic exchange-like behavior [37]. In this situation, tetracycline degradation performance is ameliorated. On the contrary, when the electrons in the anode material are not spin-polarized, the reaction process will encounter high energy barrier. In the example shown in Fig. 5(B)-(b), the reaction between tetracycline molecule (R) and M=O requires flipping the spin state of one electron to form a O-R bond, presenting a high energy barrier situation, which is not beneficial for the degradation of tetracycline. Hence, the above magnetic field enhanced electrocatalytic degradation performance of tetracycline by magnetic porous carbonized phthalonitrile resins is possible associated with the spin-selective electron removal process on the anode materials. Additionally, according to the report, the higher magnetic field strength could realize the stronger spin polarization effect during the catalytic process in superparamagnetic materials [38]. As mentioned above in part 3.1, the magnetic porous carbonized phthalonitrile resins exhibit a superparamagnetic property. Therefore, with increasing magnetic field strength, the spin polarization effect is promoted, leading an increased electrocatalytic degradation of tetracycline. Moreover, the charge transfer of the magnetic porous carbonized phthalonitrile resin is evaluated in Supporting Information, Fig. S14-S15. The electrochemical impedance spectroscopy (EIS) results indicate that the charge transfer resistance of the sample is 61.09 Ω (without magnetic field) and 46.92 Ω (with the magnetic field of 200 mT), respectively, suggesting the enhanced electron transfer kinetics under the external magnetic field [39]. Furthermore, the promoting effect of magnetohydrodynamics (MHD) like Lorentz force, Kelvin force, and Maxwell stress effect, *etc*. on the electrocatalytic degradation of tetracycline under the action of an external magnetic field might also make the contributions [40,41].

In order to further explore the degradation pathway of tetracycline, the products of electrocatalytic degradation in 20 mL of 100 mg L^{-1}

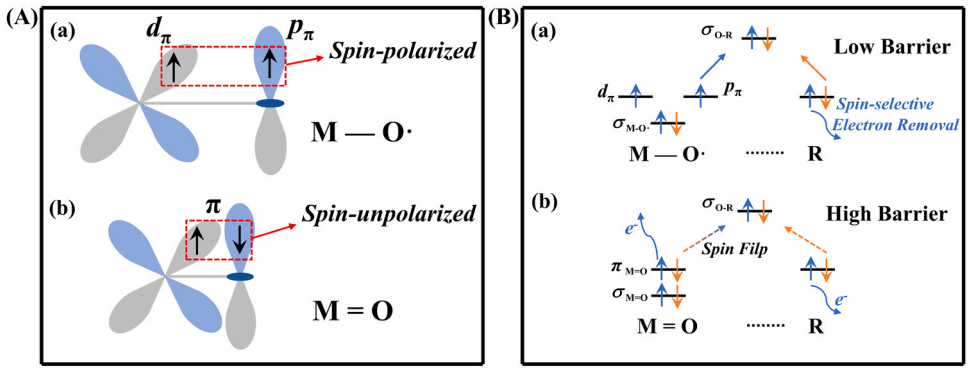

Fig. 5. . (A) Spin configurations of (a) M-O·and (b) M=O species; (B) spin-related electrocatalytic reaction of (a) low barrier process and (b) high barrier process.

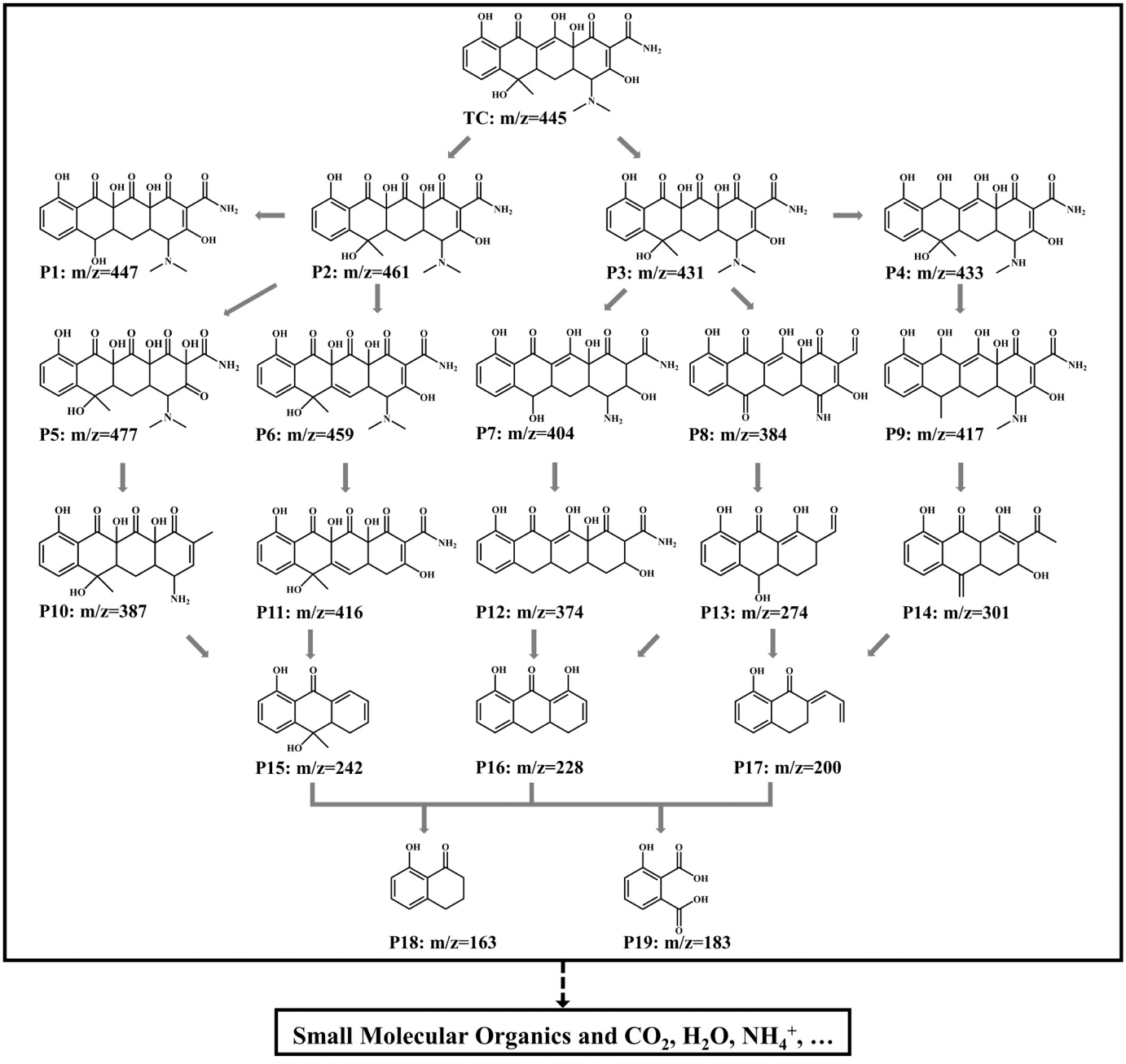

Fig. 6. Proposed pathway for the electrocatalytic degradation of tetracycline by 40BPM850 under a magnetic field of 200 mT.

tetracycline solution by 40BPM850 modified electrode for 4 h with and without magnetic field are detected by HPLC-MS and the chromatogram results are illustrated in the Fig. S16. It is noted that the main peak ($m/z = 445.1$) in the base peak chromatography (BPC) of three solutions (*i.e.*, the original tetracycline solution, tetracycline solution after degradation for 4 h with and without magnetic field) belongs to the tetracycline molecule. The products analyzed based on MS spectrometry are recorded in Table S9, and a possible degradation pathway under an external magnetic field of 200 mT has been comprehensively proposed, as presented in Fig. 6. Generally, the electron-rich groups such as dimethyl amino group, phenolic group and conjugated double bond in tetracycline are more likely to be attacked by radicals [42]. The double bonds on the ring could be attacked by M-O· and M(OH·), so that P2 and P5 are detected in MS and the adjacent hydroxyl group is oxidized to carbonyl groups. For another degradation pathway, dimethylamino group undergoes demethylation process to obtain P3. Meanwhile, demethylation and dehydroxylation may also occur to generate P1, P7 and P9. Then, P4, P9 and P10 to P14 are produced by deamination, dehydroxylation, dehydroxycarbonylation, demethylamination, and deaminocarbonylation. Subsequently, the ring structure is further opened to gain P15 to P17. In the end, more ring structures are destroyed to obtain P18 and P19. Owing to the limit of MS, the successive products are almost impossible to be detected. Notwithstanding, in accordance with decreased TOC results as mentioned above, it can be inferred that there are still some small organic molecules left and some of them are completely mineralized into CO_2, H_2O, NH_4^+. Conversely, the MS results without magnetic field indicate that the only degradation products with relatively larger molecular weights are detected, as disclosed in Fig. S17 and Table S10. This suggests that the application of magnetic field could promote the progress of electrocatalytic degradation reaction for tetracycline within the same degradation time, which is consistent with the difference of tetracycline DP% with and without magnetic field in Fig. 3 (C).

4. Conclusions

In summary, a novel magnetic porous carbonized phthalonitrile resin annealed from the mixture of MPN, polyaniline coated barium ferrite and KOH is reported, and the electrocatalytic degradation performances of tetracycline by the as-prepared samples under the external magnetic field are comprehensively evaluated. Considering the influence of magnetic field on tetracycline DP%, the optimal preparation condition corresponds to the barium ferrite loading level of 40 wt% and the annealing temperature of 850 ℃. Additionally, under such preparation condition, the tetracycline (20 mg L^{-1}) DP% significantly increases up to 37.42% with increasing the magnetic field strength from 0 to 200 mT. The optimum parameters for the electrocatalytic degradation of tetracycline under an external magnetic field of 200 mT by 40BPM850 are detected to be a bias voltage of 1.0 V (*vs.* SCE) and a pH value of 5.0. After 10 recycling times under the magnetic field of 200 mT, the tetracycline (10 mg L^{-1}) DP% slightly decreases from 95.15 % to 83.00 %, exhibiting a relatively good reusability. Particularly, the possible magnetic field enhanced electrocatalytic degradation mechanism is attributed to the spin-selective electron removal process of the reaction between metal-oxygen (MO) species and tetracycline on the anode. The comparison of degradation pathways for tetracycline with and without magnetic field verifies the improvement of tetracycline DP%. This magnetic field enhanced electrocatalytic degradation process is expected to be applied to the treatment of antibiotics in wastewater.

CRediT authorship contribution statement

Junling Zeng: Investigation, Formal analysis, Writing – original draft. **Wenhao Xie:** Formal analysis, Software. **Ying Guo:** Formal analysis, Software, Funding acquisition. **Tong Zhao:** Formal analysis, Writing – review & editing. **Heng Zhou:** Methodology, Supervision, Conceptualization. **Qiaoying Wang:** Formal analysis, Funding acquisition. **Handong Li:** Formal analysis. **Zhanhu Guo:** Writing – review & editing. **Ben Bin Xu:** Writing – review & editing. **Hongbo Gu:** Conceptualization, Funding acquisition, Supervision, Writing - review & editing.

Declaration of Competing Interest

The authors declare that they have no known competing financial interests or personal relationships that could have appeared to influence the work reported in this paper.

Data availability

Data will be made available on request.

Acknowledgments

The authors are grateful for the support from Fundamental Research Funds for the Central Universities and the Foundation of National Natural Science Foundation of China (No. 52003272). This work is supported by Shanghai Science and Technology Commission (19DZ2271500).

Appendix A. Supporting information

Supplementary data associated with this article can be found in the online version at doi:10.1016/j.apcatb.2023.123225.

References

[1] P. Sun, S. Zhou, Y. Yang, S. Liu, Q. Cao, Y. Wang, T. Wågberg, G. Hu, Artificial chloroplast-like phosphotungstic acid - iron oxide microbox heterojunctions penetrated by carbon nanotubes for solar photocatalytic degradation of tetracycline antibiotics in wastewater, Adv. Compos. Hybrid Mater. 5 (2022) 3158–3175.
[2] S. Yang, Y. Feng, D. Gao, X. Wang, N. Suo, Y. Yu, S. Zhang, Electrocatalysis degradation of tetracycline in a three-dimensional aeration electrocatalysis reactor (3D-AER) with a flotation-tailings particle electrode (FPE): Physicochemical properties, influencing factors and the degradation mechanism, J. Hazard. Mater. 407 (2021), 124361.
[3] M. Jia, Q. Liu, W. Xiong, Z. Yang, C. Zhang, D. Wang, Y. Xiang, H. Peng, J. Tong, J. Cao, H. Xu, Ti^{3+} self-doped TiO_2 nanotubes photoelectrode decorated with Ar-Fe_2O_3 derived from MIL-100(Fe): Enhanced photo-electrocatalytic performance for antibiotic degradation, Appl. Catal. B 310 (2022), 121344.
[4] X. Zuo, C. Qian, S. Ma, J. Xiong, Sulfonamide antibiotics sorption by high silica ZSM-5: Effect of pH and humic monomers (vanillin and caffeic acid), Chemosphere 248 (2020), 126061.
[5] A. Reis, B. Kolvenbach, O. Nunes, P. Corvini, Biodegradation of antibiotics: the new resistance determinants - part I, N. Biotechnol. 54 (2020) 34–51.
[6] C. Bai, G. Yang, S. Zhang, S. Deng, Y. Zhang, C. Chen, J. He, M. Xu, L. Long, A synergistic system of electrocatalytic-anode/alpha-MnO_2/peroxymonosulfate for removing combined pollution of tetracycline and Cr(VI), Chem. Eng. J. 423 (2021), 130284.
[7] S. Ahmadi, M. Kalaee, O. Moradi, F. Nosratinia, M. Abdouss, Core-shell activated carbon-ZIF-8 nanomaterials for the removal of tetracycline from polluted aqueous solution, Adv. Compos. Hybrid Mater. 4 (2021) 1384–1397.
[8] S. Wu, Y. Hu, A comprehensive review on catalysts for electrocatalytic and photoelectrocatalytic degradation of antibiotics, Chem. Eng. J. 409 (2021), 127739.
[9] J. Cai, M. Zhou, X. Xu, X. Du, Stable boron and cobalt co-doped TiO_2 nanotubes anode for efficient degradation of organic pollutants, J. Hazard. Mater. 396 (2020), 122723.
[10] S. Luo, K. Elouarzaki, Z. Xu, Electrochemistry in magnetic fields, Angew. Chem. Int. Ed. 61 (2022), e202203564.
[11] Y. Sun, X. Ren, S. Sun, Z. Liu, S. Xi, Z. Xu, Engineering high-spin state cobalt cations in spinel zinc cobalt oxide for spin channel propagation and active site enhancement in water oxidation, Angew. Chem. Int. Ed. 60 (2021) 14536–14544.
[12] H. Pan, X. Jiang, X. Wang, Q. Wang, M. Wang, Y. Shen, Effective magnetic field regulation of the radical pair spin states in rlectrocatalytic CO_2 reduction, J. Phys. Chem. Lett. 11 (2020) 48–53.
[13] H. Gu, C. Gao, A. Du, Y. Guo, H. Zhou, T. Zhao, N. Naik, Z. Guo, An overview of high-performance phthalonitrile resins: fabrication and electronic applications, J. Mater. Chem. C 10 (2022) 2925–2937.
[14] Z. Weng, K. Zhang, Y. Qi, T. Zhang, M. Xia, F. Hu, S. Zhang, C. Liu, J. Wang, X. Jian, Scalable fabrication of heteroatom-doped versatile hierarchical porous

carbons with an all-in-one phthalonitrile precursor and their applications, Carbon 159 (2020) 495–503.
[15] C. Gao, H. Gu, A. Du, H. Zhou, D. Pan, N. Naik, Z. Guo, Polyaniline facilitated curing of phthalonitrile resin with enhanced processibility and mechanical property, Polymer 219 (2021), 123533.
[16] Y. Han, D. Tang, G. Wang, Y. Guo, H. Zhou, W. Qiu, T. Zhao, Low melting phthalonitrile resins containing methoxyl and/or allyl moieties: synthesis, curing behavior, thermal and mechanical properties, Eur. Polym. J. 111 (2019) 104–113.
[17] T. Liu, L. Liang, D. Raabe, L. Dai, The martensitic transition pathway in steel, J. Mater. Sci. Technol. 134 (2023) 244–253.
[18] H. Zhao, L. Qian, Y. Chen, Q. Wang, G. Zhao, Selective catalytic two-electron O_2 reduction for onsite efficient oxidation reaction in heterogeneous electro-Fenton process, Chem. Eng. J. 332 (2018) 486–498.
[19] W. Xie, Y. Shi, Y. Wang, Y. Zheng, H. Liu, Q. Hu, S. Wei, H. Gu, Z. Guo, Electrospun iron/cobalt alloy nanoparticles on carbon nano fibers towards exhaustive electrocatalytic degradation of tetracycline in wastewater, Chem. Eng. J. 405 (2021), 126585.
[20] W. Li, Y. Wang, J. Chen, N. Hou, Y. Li, X. Liu, R. Ding, G. Zhou, Q. Li, X. Zhou, Y. Mu, Boosting photo-Fenton process enabled by ligand-to-cluster charge transfer excitations in iron-based metal organic framework, Appl. Catal. B 302 (2022), 120882.
[21] G. Qi, Y. Liu, L. Chen, P. Xie, D. Pan, Z. Shi, B. Quan, Y. Zhong, C. Liu, R. Fan, Z. Guo, Lightweight Fe_3C@Fe/C nanocomposites derived from wasted cornstalks with high-efficiency microwave absorption and ultrathin thickness, Adv. Compos. Hybrid, Adv. Compos. Hybrid Mater. 4 (2021) 1226–1238.
[22] J. Meng, Z. Cui, X. Yang, S. Zhu, Z. Li, K. Qi, L. Zheng, Y. Liang, Cobalt-iron (oxides) water oxidation catalysts: tracking catalyst redox states and reaction dynamic mechanism, J. Catal. 365 (2018) 227–237.
[23] M. Yuan, X. Feng, T. Yan, J. Chen, X. Ma, P. Cunha, S. Lan, Y. Li, H. Zhou, Y. Wang, Superparamagnetic iron oxide-enclosed hollow gold nanostructure with tunable surface plasmon resonances to promote near-infrared photothermal conversion, Adv. Compos. Hybrid. Mater. 5 (2022) 2387–2398.
[24] C. Gao, M. Yang, W. Xie, H. Zhang, H. Gu, A. Du, Z. Shi, Y. Guo, H. Zhou, Z. Guo, Adjustable magnetoresistance in semiconducting carbonized phthalonitrile resin, Chem. Commun. 57 (2021) 9894–9897.
[25] J. Zeng, W. Xie, H. Zhou, T. Zhao, B. Xu, Q. Jiang, H. Algadi, Z. Zhou, H. Gu, Nitrogen-doped graphite-like carbon derived from phthalonitrile resin with controllable negative magnetoresistance and negative permittivity, Adv. Compos. Hybrid. Mater. 6 (2023) 64.
[26] Y. Dai, Y. Yao, M. Li, X. Fang, C. Shen, F. Li, Y. Liu, Carbon nanotube filter functionalized with MIL-101(Fe) for enhanced flow-through electro-Fenton, Environ. Res. 204 (2022), 112117.
[27] T. Bui, P. Bansal, B. Lee, T. Mahvelati-Shamsabadi, T. Soltani, Facile fabrication of novel Ba-doped g-C_3N_4 photocatalyst with remarkably enhanced photocatalytic activity towards tetracycline elimination under visible-light irradiation, Appl. Surf. Sci. 506 (2020), 144184.
[28] A. Ansari, D. Nematollahi, Convergent paired electrocatalytic degradation of p-dinitrobenzene by Ti/SnO_2-Sb/beta-PbO_2 anode. A new insight into the electrochemical degradation mechanism, Appl. Catal. B 261 (2020), 118226.
[29] F. Garces-Pineda, M. Blasco-Ahicart, D. Nieto-Castro, N. Lopez, J. Galan-Mascaros, Direct magnetic enhancement of electrocatalytic water oxidation in alkaline media, Nat. Energy 4 (2019) 519–525.
[30] A. Isari, M. Mehregan, S. Mehregan, F. Hayati, R. Kalantary, B. Kakavandi, Sono-photocatalytic degradation of tetracycline and pharmaceutical wastewater using WO_3/CNT heterojunction nanocomposite under US and visible light irradiations: a novel hybrid system, J. Hazard. Mater. 390 (2020), 122050.
[31] H. Wang, T. Chen, D. Chen, X. Zou, M. Li, F. Huang, F. Sun, C. Wang, D. Shu, H. Liu, Sulfurized oolitic hematite as a heterogeneous Fenton-like catalyst for tetracycline antibiotic degradation, Appl. Catal. B 260 (2020), 118203.
[32] L. Xu, H. Zhang, P. Xiong, Q. Zhu, C. Liao, G. Jiang, Occurrence, fate, and risk assessment of typical tetracycline antibiotics in the aquatic environment: a review, Sci. Total Environ. 753 (2021), 141975.
[33] H. Gu, W. Xie, A. Du, D. Pan, Z. Guo, Overview of electrocatalytic treatment of antibiotic pollutants in wastewater, Catal. Rev. Sci. Eng. 65 (2021) 569–619.
[34] Z. Li, W. Xie, F. Yao, A. Du, Q. Wang, Z. Guo, H. Gu, Comprehensive electrocatalytic degradation of tetracycline in wastewater by electrospun perovskite manganite nanoparticles supported on carbon nanofibers, Adv. Compos. Hybrid. Mater. 5 (2022) 2092–2105.
[35] T. Wu, Z. Xu, Oxygen evolution in spin-sensitive pathways, Curr. Opin. Electrochem. 30 (2021), 100804.
[36] T. Wu, X. Ren, Y. Sun, S. Sun, G. Xian, G. Scherer, A. Fisher, D. Mandler, J. Ager, A. Grimaud, J. Wang, C. Shen, H. Yang, J. Gracia, H. Gao, Z. Xu, Spin pinning effect to reconstructed oxyhydroxide layer on ferromagnetic oxides for enhanced water oxidation, Nat. Commun. 12 (2021) 3634.
[37] J. Gracia, Itinerant spins and bond lengths in oxide electrocatalysts for oxygen evolution and reduction reactions, J. Phys. Chem. C 123 (2019) 9967–9972.
[38] Y. Li, Z. Wang, Y. Wang, A. Kovacs, C. Foo, R. Dunin-Borkowski, Y. Lu, R. Taylor, C. Wu, S. Tsang, Local magnetic spin mismatch promoting photocatalytic overall water splitting with exceptional solar-to-hydrogen efficiency, Energy Environ. Sci. 15 (2022) 265–277.
[39] O. Garcia-Rodriguez, Y. Lee, H. Olvera-Vargas, F. Deng, Z. Wang, O. Lefebvre, Mineralization of electronic wastewater by electro-Fenton with an enhanced graphene-based gas diffusion cathode, Electrochim. Acta 276 (2018) 12–20.
[40] X. Jiang, Y. Chen, X. Zhang, F. You, J. Yao, H. Yang, B. Xia, Magnetic field-assisted construction and enhancement of electrocatalysts, ChemSusChem 15 (2022), e202201551.
[41] Y. Zhang, C. Liang, J. Wu, H. Liu, B. Zhang, Z. Jiang, S. Li, P. Xu, Recent advances in magnetic field-enhanced electrocatalysis, ACS Appl. Energy Mater. 3 (2020) 10303–10316.
[42] K. Gao, L. Hou, X. An, D. Huang, Y. Yang, BiOBr/MXene/gC_3N_4 Z-scheme heterostructure photocatalysts mediated by oxygen vacancies and MXene quantum dots for tetracycline degradation: Process, mechanism and toxicity analysis, Appl. Catal. B 323 (2023), 122150.